

Sadovskii vortex in a wedge and the associated Riemann-Hilbert problem on a torus*

Y.A. ANTIPOV AND A.Y. ZEMLYANOVA

Department of Mathematics, Louisiana State University
Baton Rouge, LA 70803, USA

Department of Mathematics, Kansas State University
Manhattan, KS 66506, USA

Abstract

Reconstruction of conformal mappings from canonical slit domains onto multiply-connected physical domains with a free boundary is of interest in many different models arising in fluid mechanics. In the present paper, an exact formula for the conformal map from the exterior of two slits onto the doubly connected flow domain is obtained when a fluid flows in a wedge about a Sadovskii vortex. The map is employed to determine the potential flow outside the vortex and the vortex domain boundary provided the circulation Γ around the vortex and constant speed U on the vortex boundary are prescribed, and there are no stagnation points on the walls. The map is expressed in terms of a rational function on an elliptic surface topologically equivalent to a torus and the solution to a symmetric Riemann-Hilbert problem on a finite and a semi-infinite segments on the same genus-1 Riemann surface. Owing to its special features, the Riemann-Hilbert problem requires a novel analogue of the Cauchy kernel on an elliptic surface. Such a kernel is proposed and employed to derive a closed-form solution to the Riemann-Hilbert problem and the associated Jacobi inversion problem. The final formula for the conformal map possesses a free geometric parameter and two model parameters, the wedge angle α and Γ/U . It is shown that when $\alpha < \pi$ the solution exists and the vortex has two cusps, while the solution does not exist when the wedge angle exceeds π .

1 Introduction

Free boundary problems have attracted considerable attention because of their challenge and numerous applications including Hele-Shaw flow [11], supercavitating flow [6], flow around vortex patches [16], inverse elastic problems of inclusions whose stress field is prescribed [10], hypersonic flow in air around a body when a realistic model requires to determine shock shapes, the boundary layer, the recirculation region, and the wake behind the body [17].

In this paper we further advance the method of the Riemann-Hilbert problem on Riemann surfaces for conformal maps of multiply connected free boundary domains [2, 4], to solve a free boundary problem of vortex dynamics that concerns steady-state two-dimensional flow of a fluid in a wedge with impenetrable walls when the fluid contains a free boundary vortex domain, and there are no stagnation points on the walls.

A number of studies concern potential flows around a vortex patch defined [16] as a connected region of finite area containing uniform vorticity, surrounded by irrotational fluid. If the fluid inside a patch is at rest, then the patch is named as a hollow vortex. Its boundary is a streamline, and pressure on the boundary is constant. In one of the first studies on this subject Pocklington [14]

*The research was partly supported by EPSRC grant no EP/R014604/1 and the Simons Foundation grants no. 319217 and 713080.

solved a two-dimensional problem of uniform flow of a fluid with a pair of hollow vortices of the same area and the circulations of opposite signs. The problem of a linear array of hollow vortices in an inviscid incompressible fluid when each vortex has a fore-and-aft symmetry was solved in [7]. A model of flow around a hollow vortex placed in a corner was recently analyzed [8] by the method of conformal mappings based on the use of the Schottky-Klein prime function [9]. Since the solution to the problem of a point vortex in a corner [8] has a stagnation point on each side of the corner, the model of a hollow vortex also admits a stagnation point on each side of the corner. Such a model naturally results in the presence of a streamline that is orthogonal to the walls at the stagnation points and separates the flow into two not mixing regions, a bounded corner region with the hollow vortex inside and the external region.

Sadovskii [15] considered the problem of splicing of a vortex flow symmetric with respect to the x -axis in a potential flow without rigid boundaries when the length (not the actual profile) of the vortex domain is prescribed, $-1 \leq x \leq 1$, with the vortex distribution $\omega(x, y) = -\Omega_0 \operatorname{sgn} y$, Ω_0 is a positive constant. Two nonlinear equations for the vortex sheet strength and the vortex profile function $y = f(x)$ were derived and solved numerically. The solution [15] shows that the streamline along the x -axis branches at the points $x = \pm 1$ and forms two cusps at the branch points. A Batchelor flow in a half-plane around a Sadovsky vortex attached to the wall and a rotational right-angle corner flow was examined in [13]. In both cases the flow is separated by a vortex sheet that is also a dividing streamline. The separated streamline is attached smoothly to the wall forming cusps at the attachment points. Using a Fourier series representation of the shape with a cuspidal behavior built in they recovered numerically the flow characteristics in both divided flow regions.

In our model of the flow in a wedge around a Sadovskii vortex (Fig 1a), it is assumed that the velocity magnitude equals a constant, U , on the whole vortex boundary. In general, the tangential velocity is discontinuous across the vortex boundary, and the boundary itself is a vortex sheet. Similarly to [15], in the vortex flow domain, there is a line (Fig. 1b) that separates the vortex domain into two subdomains not necessarily of the same area with opposite circulations. We do not determine the flow inside the vortex domain. On assuming that the constant speed U and the circulation, Γ , around the vortex boundary that is a branched streamline are prescribed and nonzero we determine the vortex boundary. The problem of the irrotational flow in the wedge exterior to the vortex is exactly solved by constructing the conformal mapping from the exterior of two cuts, $l_0 = [m, \infty)$ and $l_1 = [0, 1]$, onto the flow domain. Here, m is a free parameter, and $m > 1$. The semi-infinite cut is mapped onto the boundary of the wedge, the wedge vertex is the image of some point a on the lower side of the contour l_0 , whilst the finite cut is mapped onto the boundary of the vortex domain. The conformal mapping is presented in terms of two functions. One of them is a rational function on an elliptic surface \mathcal{R} topologically equivalent to a torus. The second one is the solution to a symmetric Riemann-Hilbert problem on the same Riemann surface \mathcal{R} . Solutions to Riemann-Hilbert problems on genus-0, 1 and 2 Riemann surfaces were used [2, 3, 4, 5, 18] to reconstruct the conformal mappings associated with supercavitating flows in simply, doubly, and triply-connected domains. It turns out that the Weierstrass analogue of the Cauchy kernel [19] employed in these studies of supercavitating flows is not applicable to the Riemann-Hilbert problem arising in the vortex problem in a wedge. The reason is that the Weierstrass kernel is not sufficiently decaying at infinity with respect to the variable of integration, and its use leads to divergent integrals. We propose a new analogue of the Cauchy kernel on a hyperelliptic surface with the properties needed. In the elliptic case, this kernel is bounded at infinity and has simple poles at two bounded points of the surface. These poles generate unacceptable essential singularities of the factorization function. They are removed by solving the associated Jacobi inversion problem. The factorization of the coefficient of the Riemann-Hilbert problem is further used to derive the general solution to the Riemann-Hilbert problem that possesses a rational function on the surface

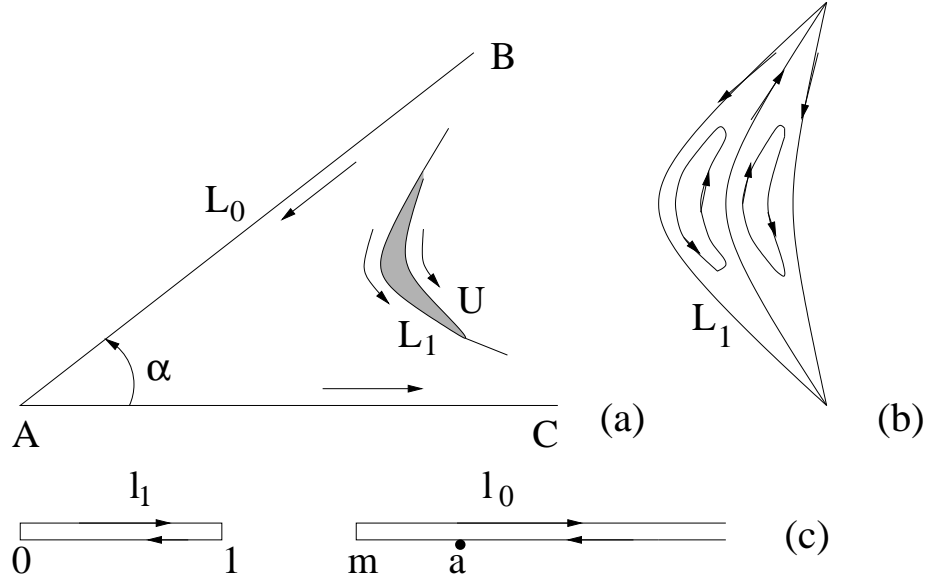


Figure 1: (a): Potential flow in a wedge around a Sadovskii vortex. (b): Mechanism of flow in the vortex. (c): Preimages of the vortex and the wedge boundaries in the parametric plane.

\mathcal{R} . By satisfying the additional conditions we arrive at a real transcendental equation with respect to the preimage a of the wedge vertex and the parameter m . It turns out that, when the infinite point of the cut l_0 falls into the infinite point of the wedge, the parameter $a = m$. This gives rise to a family of conformal mappings possessing the free geometric parameter m and two problem parameters, the wedge angle α and Γ/U .

This paper is organized as follows. In Section 2, we state the problem of a Sadovskii vortex in a wedge and express the conformal map through two functions, $\omega_0(\zeta)$ and $\omega_1(\zeta)$. In Section 3, we determine the function $\omega_0(\zeta)$. We derive and solve the Riemann-Hilbert problem on the elliptic surface \mathcal{R} for the function $\omega_1(\zeta)$ in Section 4. The exact formula for the conformal map is presented in Section 5. We employ this map to reconstruct the vortex and the wedge boundaries and report the numerical results in Section 6.

2 Model problem formulation and a conformal mapping

We consider the following two-dimensional problem of fluid dynamics.

Let an inviscid incompressible fluid flow in a wedge $\mathcal{W} = \{z \in \mathbb{C} : 0 < |z| < \infty, 0 < \arg z < \alpha\}$ whose boundary L_0 is formed by rigid impenetrable walls $AC = \{z \in \mathbb{C} : z = r > 0\}$ and $AB = \{z \in \mathbb{C} : z = re^{i\alpha}, r > 0, 0 < \alpha \leq 2\pi\}$. Suppose that in the flow domain there is a vortex \mathcal{P} (Fig.1a) whose boundary L_1 and exact location are unknown *a priori*. Fluid speed is assumed to be constant everywhere in the vortex boundary, $|\mathbf{v}| = U$, $z \in L_1$, the circulation around the vortex is Γ , no stagnation points on the walls are admitted, and the flow exterior to the vortex domain is irrotational. It is required to determine the vortex boundary and the flow exterior to the vortex.

The two-dimensional flow in the domain $\tilde{\mathcal{D}} = \mathcal{W} \setminus \mathcal{P}$ is characterized by a complex potential $w(z) = \phi(x, y) + i\psi(x, y)$ whose derivative describes the velocity vector $\mathbf{v} = (u_x, u_y)$ by $dw/dz = u_x - iu_y$, $z \in \tilde{\mathcal{D}}$. Here, ϕ is the velocity potential and ψ is the stream function. The potential $w(z)$ is an analytic multi-valued function in the flow domain with a cyclic period Γ ,

$$\int_{L_1} \frac{dw}{dz} dz = \Gamma, \quad (2.1)$$

and satisfies the following boundary conditions. On the wedge walls they are

$$\arg \frac{dw}{dz} = \begin{cases} \pi - \alpha, & z \in AB, \\ 0, & z \in AC, \end{cases} \quad \text{Im } w = c_0 = \text{const}, \quad z \in L_0. \quad (2.2)$$

These conditions mean that our model excludes the presence of stagnation points on the upper and lower boundaries of the wedge. Otherwise, if they were enforced, then $\arg dw/dz$ would be a piecewise constant function on the boundary. For example, if $r = b \in (0, +\infty)$ were a stagnation point on the lower boundary AC and the velocity direction as $r \rightarrow \infty$ is the same as in Fig.1, then $\arg dw/dz$ would be 0 for $r > b$ and π for $0 < r < b$.

The boundary L_1 of the vortex is a streamline, $\psi(x, y) = c_1 = \text{const}$, $z \in L_1$, and since the flow speed $|dw/dz|$ is a constant U , the boundary conditions on the vortex boundary read

$$\text{Im } w = c_1, \quad \left| \frac{dw}{dz} \right| = U, \quad z \in L_1. \quad (2.3)$$

At large distances, the complex potential behaves as

$$w(z) \sim \frac{\Gamma}{2\pi i} \log z + Cz^\beta, \quad z \rightarrow \infty, \quad z \in \tilde{\mathcal{D}}, \quad (2.4)$$

where $\beta > 0$ is a parameter to be determined, and C is a constant.

The vortex flow inside the vortex domain is characterized similarly to the Sadvskii model [15]. A streamline branches at some interior point in the wedge, the two branches merge at another point, and a finite region is formed. At these two points, the streamline branches form cusps. Otherwise, if the cusps are excluded, two inadmissible stagnation points in the vortex boundary have to be enforced. The presence of the cusps will be also confirmed numerically. The vortex domain itself is divided into two subdomains with vortex distributions of different sign (Fig. 1b). Apart from the condition (2.1) that prescribes the circulation around the vortex, owing to the second condition in (2.3) and the Bernoulli's equation, we know that the pressure distribution is constant on the vortex boundary. In addition, we remark that the conditions (2.3) do not rule out a possible discontinuity of the tangential velocity across the vortex boundary. In this case the boundary is a vortex sheet, and as in [15], the Bernoulli constant jumps across the vortex boundary.

To deal with the problem, consider another complex plane, a ζ -plane, cut along two segments, $l_0 = [m, +\infty)$ ($m > 1$) and $l_1 = [0, 1]$ (Fig. 1c). Denote the exterior of these two slits by \mathcal{D} . Let $z = f(\zeta)$ be a conformal map of this doubly connected domain onto the flow domain $\tilde{\mathcal{D}}$. We assume that the function $f(\zeta)$ maps the slits l_0 and l_1 onto the wedge and vortex boundaries L_0 and L_1 , respectively. The positive directions of the contours l_0 and l_1 are chosen to be consistent with those in the physical domain — when a point ζ traverses the contours, the domain \mathcal{D} is seen on the left. Since the direction of l_1 corresponds to the negative direction of the contour L_1 with respect to the interior of the vortex domain, the circulation $\Gamma < 0$. For the upper and lower sides of the contours l_0 and l_1 , we shall use the notations l_0^\pm and l_1^\pm , respectively. We choose the map such that the infinite point $\zeta = \infty \in \mathcal{D}$ falls into the infinite point of the flow domain, $z = \infty \in \tilde{\mathcal{D}}$. Without loss, it is assumed that the preimage of the wedge vertex A is a point a lying in the lower side of the semi-infinite cut including the point m . This assumption inevitably gives us the preimages of the points B and C in the parametric plane: they are $+\infty - i0$ and $+\infty + i0$, respectively.

In order to reconstruct the conformal mapping, we express the derivative $f'(\zeta)$ through the derivative dw/dz and the logarithmic hodograph variable as

$$\frac{df}{d\zeta} = \omega_0(\zeta)e^{-\omega_1(\zeta)}, \quad (2.5)$$

where

$$\omega_0(\zeta) = \frac{dw}{U d\zeta}, \quad \omega_1(\zeta) = \log \frac{dw}{U dz}. \quad (2.6)$$

3 Function $\omega_0(\zeta)$ and asymptotics of the map

Since the imaginary part of the function $w(z)$ is constant on L_0 and L_1 , we have $\text{Im } dw/d\zeta = 0$ on the contours l_0 and l_1 . In virtue of (2.6) the function $\omega_0(\zeta)$ is analytic in the domain $\mathcal{D} = \mathbb{C} \setminus (l_0 \cup l_1)$, satisfies the boundary condition

$$\text{Im } \omega_0(\xi) = 0, \quad \xi \in l_0 \cup l_1, \quad (3.1)$$

and may have integrable singularities at the finite endpoints of the contours l_0 and l_1 . At infinity, $\omega_0(\zeta) = O(\zeta^{-\mu})$ with $\mu > 0$. The most general form of such a function is

$$\omega_0(\zeta) = \frac{i(N_0 + N_1\zeta)}{p^{1/2}(\zeta)}, \quad (3.2)$$

where N_0 and N_1 are arbitrary real constants, and

$$p(\zeta) = \zeta(1 - \zeta)(\zeta - m). \quad (3.3)$$

The function $p^{1/2}(\zeta)$ is analytic in the ζ -plane cut along the lines l_0 and l_1 . Its single branch is fixed by the condition $p^{1/2}(\zeta) = i\sqrt{|p(\xi)|}$ as $\zeta = \xi + i0$, $\xi > m$. This branch has the following properties:

$$\begin{aligned} p^{1/2}(\zeta) &= \pm i\sqrt{|p(\xi)|}, \quad \zeta = \xi \pm i0, \quad m < \xi < +\infty, \\ p^{1/2}(\zeta) &= -\sqrt{|p(\xi)|}, \quad \zeta = \xi, \quad 1 < \xi < m, \\ p^{1/2}(\zeta) &= \mp i\sqrt{|p(\xi)|}, \quad \zeta = \xi \pm i0, \quad 0 < \xi < 1, \\ p^{1/2}(\zeta) &= \sqrt{|p(\xi)|}, \quad \zeta = \xi, \quad -\infty < \xi < 0. \end{aligned} \quad (3.4)$$

The function $\omega_0(\zeta)$ is bounded as $\zeta \rightarrow a$ if $a \neq m$ and has the square root singularity $\omega_0(\zeta) = O((\zeta - a)^{-1/2})$ otherwise.

We next analyze the behavior of the function $f(\zeta)$ at the points $\zeta = a$ and $\zeta = \infty$. Consider a copy of the ζ -plane cut along the semi-infinite segment $l_0 = [m, \infty)$. By the map $f_1(\zeta) = \sqrt{\zeta - m}$ it is transformed into the upper half-plane with the points m and $a \in l_0^-$ being transformed into the origin and the point $-\sqrt{a - m}$, respectively. By the translation transformation $f_2(\zeta) = f_1(\zeta) + \sqrt{a - m}$ we move the point $-\sqrt{a - m}$ into the origin. Finally, by implementing the transformation $z = f_2^{\alpha/\pi}(\zeta)$, we map the upper half-plane into the wedge W in the z -plane. The composition of these three maps has the form

$$z = (\sqrt{\zeta - m} + \sqrt{a - m})^{\alpha/\pi} = \frac{(\zeta - a)^{\alpha/\pi}}{(\sqrt{\zeta - m} - \sqrt{a - m})^{\alpha/\pi}}. \quad (3.5)$$

Note that this map transforms the finite cut l_1 into a closed contour inside the wedge W . The map (3.5) and the function $f(\zeta)$ share the same asymptotics at the points a and ∞ . Consequently, if $a \neq m$, then formula (3.5) implies

$$\begin{aligned} f(\zeta) &\sim K_0(\zeta - a)^{\alpha/\pi}, \quad \zeta \rightarrow a \in l_0^-, \quad f(\zeta) \sim K_1, \quad \zeta \rightarrow \bar{a} \in l_0^+, \\ f(\zeta) &\sim \zeta^{\alpha/(2\pi)}, \quad \zeta \rightarrow \infty. \end{aligned} \quad (3.6)$$

Here, K_0 and K_1 are some constants.

In the case $a = m$, the asymptotics of the function $f(\zeta)$ at infinity is the same, whilst at the left endpoint of the cut l_0 , we have

$$f(\zeta) \sim K_0(\zeta - a)^{\alpha/(2\pi)}, \quad \zeta \rightarrow a = m. \quad (3.7)$$

4 Function $\omega_1(\zeta)$ and a Riemann-Hilbert problem on a torus

4.1 Hilbert problem for the function $\omega_1(\zeta)$

We now turn our attention to the function $\omega_1(\zeta)$. Comparing the asymptotics (2.4) and (3.6) at infinity and using formula (3.2) we deduce from (2.5) and (2.6)

$$\beta = \frac{\pi}{\alpha}, \quad \frac{dw}{Udz} \sim \frac{\pi C}{\alpha} \zeta^{(\pi-\alpha)/(2\pi)}, \quad \zeta \rightarrow \infty, \quad (4.1)$$

and therefore

$$\omega_1(\zeta) \sim \frac{\pi - \alpha}{2\pi} \log \zeta, \quad \zeta \rightarrow \infty. \quad (4.2)$$

In a similar fashion we determine the asymptotics of the function $\omega_1(\zeta)$ at the point a . If $a \neq m$ ($a \in l_0^-$), then we have

$$\frac{dw}{Udz} \sim C'(\zeta - a)^{1-\alpha/\pi}, \quad \zeta \rightarrow a, \quad \frac{dw}{Udz} \sim C'', \quad \zeta \rightarrow \bar{a}, \quad (4.3)$$

where C' and C'' are constants. The second formula in (2.6) yields

$$\omega_1(\zeta) \sim \frac{\pi - \alpha}{\pi} \log(\zeta - a), \quad \zeta \rightarrow a, \quad \omega_1(\zeta) \sim \log C'', \quad \zeta \rightarrow \bar{a}. \quad (4.4)$$

If it happens that $a = m$, then

$$\omega_1(\zeta) \sim \frac{\pi - \alpha}{2\pi} \log(\zeta - a), \quad \zeta \rightarrow a. \quad (4.5)$$

At the point \bar{a} the function $\omega_1(\zeta)$ is bounded and at infinity has the same asymptotics (4.2) as in the case $a \neq m$.

Analyze next the boundary conditions. Observe in equations (2.2) and (2.3) that the values of the argument and modulus of the function dw/dz give rise to the imaginary and real parts of the function $\omega_1(\zeta)$. We have

$$\operatorname{Im} \omega_1(\zeta) = \begin{cases} \pi - \alpha, & \zeta \in l_0', \\ 0, & \zeta \in l_0'', \end{cases} \quad \operatorname{Re} \omega_1(\zeta) = 0, \quad \zeta \in l_1. \quad (4.6)$$

Here, $l_0' = [a, +\infty)^-$, $l_0'' = [m, a]^- \cup [m, +\infty)^+$, and the superscripts $+$ and $-$ indicate that the segments belong to the upper and lower sides of the contour l_0 , correspondingly. The problem for the function $\omega_1(\zeta)$ obtained is classified as a Hilbert problem of the theory of analytic functions on two two-sided positively oriented contours (the exterior of the loops l_0 and l_1 is on the left when a point ζ traverses the contours in the positive direction). To solve this problem, we reduce it to a Riemann-Hilbert problem on two contours of a symmetric genus-1 Riemann surface topologically equivalent to a torus.

4.2 Riemann-Hilbert problem for an auxiliary function $\Phi(\zeta, u)$ on a torus

Let \mathbb{C}_1 and \mathbb{C}_2 be two copies of the extended complex ζ -plane cut along the segments $l_1 = [0, 1]$ and $l_0 = [m, +\infty)$ and \mathcal{R} be a genus-1 Riemann surface defined by the algebraic equation

$$u^2 = p(\zeta), \quad p(\zeta) = \zeta(1 - \zeta)(\zeta - m). \quad (4.7)$$

The surface is formed by gluing the two sheets together in such a way that the upper sides l_j^+ of the cuts $l_j \subset \mathbb{C}_1$ are glued to the lower sides l_j^- of the cuts $l_j \subset \mathbb{C}_2$, and the sides $l_j^- \subset \mathbb{C}_1$ are glued to $l_j^+ \subset \mathbb{C}_2$ ($j = 0, 1$). Let $p^{1/2}(\zeta)$ be the branch fixed in Section 3. Then the function $u(\zeta)$

$$u = \begin{cases} p^{1/2}(\zeta), & (\zeta, u) \in \mathbb{C}_1, \\ -p^{1/2}(\zeta), & (\zeta, u) \in \mathbb{C}_2, \end{cases} \quad (4.8)$$

is uniquely defined and single-valued on \mathcal{R} . The pairs $(\zeta, p^{1/2}(\zeta))$ and $(\zeta, -p^{1/2}(\zeta))$ correspond to the points with affix ζ lying on the upper and lower sheets, \mathbb{C}_1 and \mathbb{C}_2 , respectively. The contour $\mathcal{L} = l_0 \cup l_1$ is the symmetry line for the elliptic surface \mathcal{R} which splits the surface into two symmetric halves with symmetric points $(\zeta, u) \in \mathbb{C}_1$ and $(\zeta_*, u_*) = (\bar{\zeta}, -u(\bar{\zeta})) \in \mathbb{C}_2$.

Introduce an auxiliary function on the surface \mathcal{R}

$$\Phi(\zeta, u) = \begin{cases} -i\omega_1(\zeta), & (\zeta, u) \in \mathbb{C}_1, \\ i\omega_1(\bar{\zeta}), & (\zeta, u) \in \mathbb{C}_2. \end{cases} \quad (4.9)$$

Everywhere on the torus this function satisfies the symmetry condition

$$\overline{\Phi(\zeta_*, u_*)} = \Phi(\zeta, u), \quad (\zeta, u) \in \mathcal{R}. \quad (4.10)$$

On the symmetry line \mathcal{L} , its boundary values are expressed through the real and imaginary values of the function $\omega_1(\xi)$,

$$\begin{aligned} \Phi^+(\xi, v) &= -i\omega_1(\xi) = -i \operatorname{Re} \omega_1(\xi) + \operatorname{Im} \omega_1(\xi), \\ \Phi^-(\xi, v) &= i\overline{\omega_1(\xi)} = i \operatorname{Re} \omega_1(\xi) + \operatorname{Im} \omega_1(\xi), \quad (\xi, v) \in \mathcal{L}. \end{aligned} \quad (4.11)$$

Here and henceforth, $v = u(\xi)$, $\Phi^+(\xi, v)$ and $\Phi^-(\xi, v)$ are the limit values of the function $\Phi(\zeta, u)$ on the contour \mathcal{L} from the upper and lower sheet of the surface, respectively. On summarizing the properties of the function $\Phi(\zeta, u)$ we state the following Riemann-Hilbert problem.

Find all symmetric functions $\Phi(\zeta, u)$, $\overline{\Phi(\zeta_, u_*)} = \Phi(\zeta, u)$, $(\zeta, u) \in \mathcal{R}$, analytic in $\mathcal{R} \setminus \mathcal{L}$, Hölder-continuous up to the boundary \mathcal{L} apart from the singular points $\zeta = a$ and $\zeta = \infty$ with the boundary values satisfying the relation*

$$\Phi^+(\xi, v) = G(\xi, v)\Phi^-(\xi, v) + g(\xi, v), \quad (\xi, v) \in \mathcal{L}, \quad (4.12)$$

Here,

$$G(\xi, v) = \begin{cases} -1, & (\xi, v) \in l_0 \\ 1, & (\xi, v) \in l_1, \end{cases} \quad g(\xi, v) = \begin{cases} 2(\pi - \alpha), & (\xi, v) \in l'_0, \\ 0, & (\xi, v) \in l''_0, \\ 0, & (\xi, v) \in l_1. \end{cases} \quad (4.13)$$

The function $\Phi(\zeta, u)$ has a logarithmic singularity at the infinite point (∞, ∞) ,

$$\Phi(\zeta, u) \sim \frac{\pi - \alpha}{2\pi i} \log \zeta, \quad \zeta \rightarrow \infty, \quad (4.14)$$

It is bounded at the point $(\bar{a}, u(\bar{a}))$ and has a logarithmic singularity at the point $(a, u(a))$,

$$\Phi(\zeta, u) \sim \frac{\pi - \alpha}{\sigma \pi i} \log(\zeta - a), \quad \zeta \rightarrow a, \quad (4.15)$$

where $\sigma = 1$ if $a \neq m$ and $\sigma = 2$ otherwise.

4.3 Analogue of the Cauchy kernel

The standard solution device for scalar Riemann-Hilbert problems on elliptic and hyperelliptic surfaces is the Wierstrass kernel [19], an analogue of the Cauchy kernel for Riemann surfaces. It has the form

$$dW = \frac{1}{2} \left(1 + \frac{u}{v} \right) \frac{d\xi}{\xi - \zeta}, \quad u = u(\zeta), \quad v = u(\xi). \quad (4.16)$$

This kernel is applicable if the Riemann-Hilbert problem contour is bounded or the density decays at infinity at a sufficient rate otherwise. When the contour is unbounded and the density does not decay at infinity fast enough, the employment of the kernel (4.16) gives rise to divergent integrals. In our case the contour \mathcal{L} of the Riemann-Hilbert problem comprises a finite contour l_1 and a semi-infinite contour l_0 . Since the function $g(\xi, v)$ defined in (4.13) is a nonzero constant in the contour $l'_0 = [a, \infty)^-$, we need a kernel different from the one in (4.16).

We propose to use a new analogue of the Cauchy kernel convenient for our purposes. Consider the differential

$$dV = \frac{1}{2} \left[1 + \frac{u(\xi - \zeta_0)^2}{v(\zeta - \zeta_0)^2} \right] \left(\frac{1}{\xi - \zeta} - \frac{1}{\xi - \zeta_0} \right) d\xi, \quad (4.17)$$

where ζ_0 is an arbitrary real fixed point not lying on the contours l_0 and l_1 (in our case it is convenient to select ζ_0 by the condition $\zeta_0 < 0$). Equivalently, the kernel dV may be written in the form

$$dV = \frac{1}{2} \left[\frac{\zeta - \zeta_0}{\xi - \zeta_0} + \frac{u\xi - \zeta_0}{v\zeta - \zeta_0} \right] \frac{d\xi}{\xi - \zeta}. \quad (4.18)$$

This kernel possesses the following properties.

(i) If ζ is a fixed bounded point on the torus \mathcal{R} and $\xi \rightarrow \pm i0 + \infty$, then dV is decaying as $\xi^{-3/2}$ that is

$$dV \sim \pm \frac{1}{2i} \frac{u(\zeta)}{\zeta - \zeta_0} \xi^{-3/2} d\xi, \quad \xi \rightarrow \pm i0 + \infty. \quad (4.19)$$

(ii) If ξ is a fixed point lying either in the contour l_1 or any finite part of the contour l_0 and $\zeta \rightarrow \infty$, then the kernel dV is bounded,

$$dV \sim \left[-\frac{1}{2(\xi - \zeta_0)} + O(\zeta^{-1/2}) \right] d\xi, \quad \zeta \rightarrow \infty. \quad (4.20)$$

(iii) If $\zeta \rightarrow \xi \in \mathcal{L}$, then the kernel behaves as the Cauchy kernel. Indeed, if $\zeta \in \mathbb{C}_1$ and $\zeta \rightarrow \xi$, then for $\xi \in \mathcal{L} \subset \mathbb{C}_1$

$$dV \sim \frac{d\xi}{\xi - \zeta}, \quad (4.21)$$

whilst for $\xi \in \mathcal{L} \subset \mathbb{C}_2$, $u/v \sim -1$, and the kernel dV is bounded. The analysis is similar when $\zeta \in \mathbb{C}_2$.

(iv) Since ζ_0 is a real number, the kernel dV is symmetric with respect to the symmetry contour \mathcal{L} ,

$$dV((\xi, v), (\zeta, u(\zeta))) = \overline{dV((\xi, v), (\bar{\zeta}, -u(\bar{\zeta})))}. \quad (4.22)$$

(v) At the two points of the torus with affix ζ_0 , $(\zeta_0, u(\zeta_0))$ and $(\zeta_0, -u(\zeta_0))$, the kernel dV has simple poles. They will give rise to essential singularities of the factorization function associated with the Riemann-Hilbert problem (4.12) and will have to be removed by solving a Jacobi inversion problem.

The kernel we presented can be generalized in the case of a hyperelliptic surface of any finite genus ρ . We write down such an analogue since similar problems of higher genera might arise in other applications. Let \mathcal{R} be the genus- ρ hyperelliptic surface of the algebraic function $u^2 = (\zeta -$

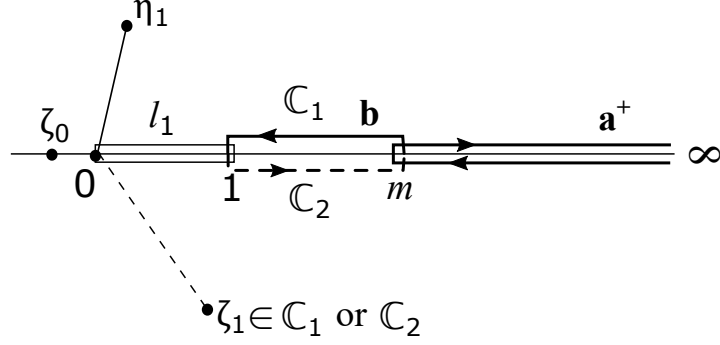


Figure 2: Canonical cross-sections and the contour $\gamma = \mathbf{p}_1 \mathbf{q}_1$, $\mathbf{p}_1 = (\eta_1, u(\eta_1)) \in \mathbb{C}_1$, and $\mathbf{q}_1 = (\zeta_1, u(\zeta_1)) \in \mathcal{R}$.

$a_1)(\zeta - a_2) \dots (\zeta - a_{2\rho+1})$ (the infinite point is a branch point) or $u^2 = (\zeta - a_1)(\zeta - a_2) \dots (\zeta - a_{2\rho+2})$ (all the branch points are finite). Then the counterpart of the kernel (4.17) has the form

$$dV = \frac{1}{2} \left[1 + \frac{u}{v} \prod_{j=0}^{\rho} \frac{\xi - \zeta_j}{\zeta - \zeta_j} \right] \left(\frac{1}{\xi - \zeta} - \frac{1}{\xi - \zeta_0} \right) d\xi. \quad (4.23)$$

Here, $\zeta_0, \dots, \zeta_{\rho}$ are arbitrary fixed not necessarily distinct points in the real axis not falling on the contour of the Riemann-Hilbert problem that is the union of the branch cuts of the Riemann surface.

4.4 Factorization problem

We aim to determine a piece-wise meromorphic function $X(\zeta, u)$ symmetric on the torus,

$$X(\zeta, u) = \overline{X(\bar{\zeta}, -u(\bar{\zeta}))}, \quad (\zeta, u) \in \mathcal{R} \setminus \mathcal{L}, \quad (4.24)$$

continuous through the contour l_1 , discontinuous through the contour l_0 , and whose boundary values on the contour satisfy the equation

$$X^+(\xi, v) = G(\xi, v) X^-(\xi, v), \quad (\xi, v) \in \mathcal{L} \subset \mathcal{R}. \quad (4.25)$$

Analyze the following function:

$$X(\zeta, u) = \chi(\zeta, u) \chi_1(\zeta, u) \overline{\chi_1(\zeta_*, u_*)}, \quad (4.26)$$

where

$$\begin{aligned} \chi(\zeta, u) &= \exp \left\{ \frac{1}{2\pi i} \oint_{l_0} \log(-1) dV \right\}, \\ \chi_1(\zeta, u) &= \exp \left\{ - \left(\int_{\gamma} +n_a \oint_{\mathbf{a}} +n_b \oint_{\mathbf{b}} \right) dV \right\}. \end{aligned} \quad (4.27)$$

The contours \mathbf{a} and \mathbf{b} constitute a system of canonical cross-sections of the surface \mathcal{R} . They are chosen as follows. The contour \mathbf{a} lies on both sheets of the surface and coincides with the banks of the semi-infinite cut l_0 (Fig.2). The loop \mathbf{b} consists of the segments $[m, 1] \subset \mathbb{C}_1$ and $[1, m] \subset \mathbb{C}_2$. The positive direction on the loop \mathbf{a} is chosen such that the upper sheet is on the left. The loop \mathbf{a} intersects the loop \mathbf{b} at the branch point $\zeta = m$ from left to the right.

The contour γ is a continuous curve whose starting and terminal points are $\mathbf{p}_1 = (\eta_1, u(\eta_1))$ and $\mathbf{q}_1 = (\zeta_1, u(\zeta_1))$, respectively. The point \mathbf{p}_1 is an arbitrary fixed point lying in either sheet of the surface. Without loss, select $\mathbf{p}_1 = (\eta_1, p^{1/2}(\eta_1)) \in \mathbb{C}_1$. As for the point \mathbf{q}_1 , it has to be determined and may fall on either sheet. The integers n_a and n_b cannot be fixed *a priori* either and are to be recovered from a condition which guarantees the boundedness of the solution to the problem (4.25) at the two points of the torus with affix ζ_0 , the simple poles of the kernel dV . The contour γ is chosen such that it does not cross the **a**- and **b**-cross-sections. In the case $\mathbf{q}_1 \in \mathbb{C}_2$, it passes through the point $\zeta = 0$, a branch point of the surface \mathcal{R} , and consists of two parts, $(\mathbf{p}_1, 0) \subset \mathbb{C}_1$ and $(0, \mathbf{q}_1) \subset \mathbb{C}_2$. If it turns out that the point \mathbf{q}_1 lies on the upper sheet, then the contour γ can be taken as the straight segment joining these points provided it does not cross the loops l_0 and l_1 . Otherwise, if the imaginary parts of the points η_1 and ζ_1 have different signs, both points \mathbf{p}_1 and \mathbf{q}_1 lie in the sheet \mathbb{C}_1 , and the straight segment $\mathbf{p}_1\mathbf{q}_1$ intersects the contour \mathcal{L} , then γ can be selected as a polygonal line consisting of two segments $\mathbf{p}_1\mathbf{p}_0$ and $\mathbf{p}_0\mathbf{q}_1$ with $\mathbf{p}_0 = (\delta, p^{1/2}(\delta))$ and $\zeta_0 < \delta < 0$.

Note that the integrals in (4.27) have jumps through the contours γ , **a**, and **b**, respectively. However, since the jumps are multiples of $2\pi i$, the functions in the right hand-side in (4.26) are continuous through these contours. It is directly verified that the function (4.26) satisfies the symmetry condition (4.24).

The integral representation of the factorization function $X(\zeta, u)$ can be simplified. By employing the Cauchy theorem we deduce

$$\chi(\zeta, u) = \exp \left\{ \frac{u(\zeta)}{4(\zeta - \zeta_0)} \oint_{l_0} \frac{(\xi - \zeta_0)d\xi}{u(\xi)(\xi - \zeta)} \right\}. \quad (4.28)$$

In the product $\chi_1(\zeta, u)\overline{\chi_1(\zeta_*, u_*)}$, the integrals over the cross-section **b** are cancelled and we have

$$\begin{aligned} \chi_1(\zeta, u)\overline{\chi_1(\zeta_*, u_*)} = \exp \left\{ -\frac{1}{2} \int_{\gamma} \left(\frac{\zeta - \zeta_0}{\xi - \zeta_0} + \frac{u(\zeta)}{u(\xi)} \frac{\xi - \zeta_0}{\zeta - \zeta_0} \right) \frac{d\xi}{\xi - \zeta} \right. \\ \left. - \frac{1}{2} \int_{\gamma} \left(\frac{\zeta - \zeta_0}{\bar{\xi} - \zeta_0} - \frac{u(\zeta)}{u(\bar{\xi})} \frac{\bar{\xi} - \zeta_0}{\zeta - \zeta_0} \right) \frac{d\bar{\xi}}{\bar{\xi} - \zeta} - \frac{n_a u(\zeta)}{\zeta - \zeta_0} \oint_{\mathbf{a}} \frac{(\xi - \zeta_0)d\xi}{u(\xi)(\xi - \zeta)} \right\}. \end{aligned} \quad (4.29)$$

Since the contour l_0 and the loop **a** have the same direction and coincide pointwise, we derive the following representation for the solution of the factorization problem:

$$\begin{aligned} X(\zeta, u) = \exp \left\{ \left(\frac{1}{2} - 2n_a \right) \frac{u(\zeta)}{i(\zeta - \zeta_0)} \int_m^\infty \frac{(\xi - \zeta_0)d\xi}{\sqrt{|p(\xi)|}(\xi - \zeta)} \right. \\ \left. - \frac{1}{2} \int_{\gamma} \left(\frac{\zeta - \zeta_0}{\xi - \zeta_0} + \frac{u(\zeta)}{u(\xi)} \frac{\xi - \zeta_0}{\zeta - \zeta_0} \right) \frac{d\xi}{\xi - \zeta} - \frac{1}{2} \int_{\gamma} \left(\frac{\zeta - \zeta_0}{\bar{\xi} - \zeta_0} - \frac{u(\zeta)}{u(\bar{\xi})} \frac{\bar{\xi} - \zeta_0}{\zeta - \zeta_0} \right) \frac{d\bar{\xi}}{\bar{\xi} - \zeta} \right\}. \end{aligned} \quad (4.30)$$

We describe the main properties of the function $X(\zeta, u)$ given by (4.30).

(i) The function $X(\zeta, u)$ satisfies the symmetry condition (4.24) and the boundary condition (4.25).

(ii) The limit values $X^+(\xi \pm i0, u^\pm(\xi))$ and $X^-(\xi \pm i0, u^\pm(\xi))$ on both sides of the contour l_0 are expressed through the Cauchy principal value of the first integral in (4.30) as

$$\begin{aligned} X^+(\xi \pm i0, u^\pm(\xi)) &= iX(\xi, u^\pm(\xi)), \quad \xi \in l_0^+. \\ X^-(\xi \pm i0, u^\pm(\xi)) &= -iX(\xi, u^\pm(\xi)), \quad \xi \in l_0^\pm. \end{aligned} \quad (4.31)$$

(iii) In virtue of the behavior of the Cauchy integral at the endpoints of the contour γ , the function $X(\zeta, u)$ has a simple zero at the point $\mathbf{p}_1 \in \mathbb{C}_1$ and a simple pole at the point $\mathbf{q}_1 \in \mathcal{R}$.

(iv) As a consequence of the poles of the kernel at the points $(\zeta_0, u(\zeta_0))$ and $(\zeta_0, -u(\zeta_0))$, the function $X(\zeta, u)$ has essential singularities at these two points. They will be removed in the next section by solving the associated Jacobi inversion problem.

4.5 Jacobi inversion problem

To remove the essential singularities of the factorization function $X(\zeta, u)$ at the points $(\zeta_0, \pm u(\zeta_0))$, we require

$$\operatorname{res}_{\zeta=\zeta_0} \frac{u(\zeta)}{\zeta - \zeta_0} \left\{ \left(\frac{1}{2} - 2n_a \right) \int_m^\infty \frac{(\xi - \zeta_0)d\xi}{i\sqrt{|p(\xi)|}(\xi - \zeta)} - \frac{1}{2} \int_\gamma \frac{(\xi - \zeta_0)d\xi}{u(\xi)(\xi - \zeta)} + \frac{1}{2} \int_\gamma \frac{(\bar{\xi} - \zeta_0)d\bar{\xi}}{u(\xi)(\bar{\xi} - \zeta)} \right\} = 0. \quad (4.32)$$

This brings us to the following nonlinear equation with respect to the point \mathbf{q}_1 , the terminal point of the contour γ , and the integer n_a :

$$\left(\frac{1}{4} - n_a \right) \oint_{\mathbf{a}} \frac{d\xi}{u(\xi)} - \frac{1}{2} \int_\gamma \frac{d\xi}{u(\xi)} + \frac{1}{2} \int_\gamma \frac{d\bar{\xi}}{u(\xi)} = 0, \quad (4.33)$$

which can be considered [4] as an imaginary analogue of the Jacobi inversion problem

$$\int_0^{\mathbf{q}_1} \frac{d\xi}{u(\xi)} + n_a \mathcal{A} + n_b \mathcal{B} = g_0, \quad (4.34)$$

where \mathcal{A} and \mathcal{B} are the \mathcal{A} - and \mathcal{B} - periods of the abelian integral

$$\int_0^{\mathbf{q}} \frac{d\xi}{u(\xi)} \quad (4.35)$$

given in terms of the Legendre complete elliptic integrals [12]

$$\begin{aligned} \mathcal{A} &= \oint_{\mathbf{a}} \frac{d\xi}{u(\xi)} = -2i \int_m^\infty \frac{d\xi}{\sqrt{|\xi(\xi-1)(\xi-m)|}} = -4ik\mathbf{K}(k), \\ \mathcal{B} &= \oint_{\mathbf{b}} \frac{d\xi}{u(\xi)} = 2 \int_1^m \frac{d\xi}{\sqrt{|\xi(\xi-1)(\xi-m)|}} = 4k\mathbf{K}'(k), \end{aligned} \quad (4.36)$$

$k = m^{-1/2}$, and

$$g_0 = -ik\mathbf{K}(k) + \int_0^{\eta_1} \frac{d\xi}{p^{1/2}(\xi)}. \quad (4.37)$$

The only one difference between the Jacobi problem (4.34) and the one solved in [4] is the right hand-side g_0 . By adjusting the formulas [4] to our case we can describe the solution procedure as follows. Compute the affix of the point \mathbf{q}_1 by

$$\zeta_1 = \operatorname{sn}^2 \frac{ig_0}{2k} \quad (4.38)$$

and evaluate the integrals

$$I_{\pm} = \int_0^{\eta_1} \frac{d\xi}{p^{1/2}(\xi)} \pm \int_0^{\zeta_1} \frac{d\xi}{p^{1/2}(\xi)} - ik\mathbf{K}(k) \quad (4.39)$$

and the numbers n_a and n_b

$$n_a = -\frac{\operatorname{Im} I_-}{4k\mathbf{K}(k)}, \quad n_b = \frac{\operatorname{Re} I_-}{4k\mathbf{K}'(k)}. \quad (4.40)$$

If both of the numbers n_a and n_b are integers, then the point \mathbf{q}_1 lies in the upper sheet \mathbb{C}_1 , $\mathbf{q}_1 = (\zeta_1, p^{1/2}(\zeta_1))$. Otherwise, $\mathbf{q}_1 \in \mathbb{C}_2$, $\mathbf{q}_1 = (\zeta_1, -p^{1/2}(\zeta_1))$, and the numbers n_a and n_b computed by the formulas

$$n_a = -\frac{\text{Im } I_+}{4k\mathbf{K}(k)}, \quad n_b = \frac{\text{Re } I_+}{4k\mathbf{K}'(k)} \quad (4.41)$$

are integers. If the point \mathbf{q}_1 and the integer n_a are determined according to this procedure, then the function $X(\zeta, u)$ is bounded at the points $(\zeta_0, \pm u(\zeta_0))$ and provides a solution to the factorization problem (4.24), (4.25).

4.6 Solution to the Riemann-Hilbert problem

First we use the factorization of the function $G(\zeta, v)$ and rewrite the boundary condition (4.12) in the form

$$\frac{\Phi^+(\xi, v)}{X^+(\xi, v)} = \frac{\Phi^-(\xi, v)}{X^-(\xi, v)} + \frac{g(\xi, v)}{X^+(\xi, v)}, \quad (\xi, v) \in \mathcal{L}. \quad (4.42)$$

Next we introduce the singular integral with the kernel dV on the torus \mathcal{R}

$$\Psi(\zeta, u) = \frac{\pi - \alpha}{2\pi i} \int_{l'_0} \left[\frac{\zeta - \zeta_0}{\xi - \zeta_0} + \frac{u(\zeta)}{u(\xi)} \frac{\xi - \zeta_0}{\zeta - \zeta_0} \right] \frac{d\xi}{(\xi - \zeta)X^+(\xi, u(\xi))}. \quad (4.43)$$

Note that this function satisfies the symmetry condition $\Psi(\zeta, u) = \overline{\Psi(\zeta_*, u_*)}$, is discontinuous through the contour l'_0 with the jump $2(\pi - \alpha)/X^+(\xi, v)$ and continuous through the contours l'_0 and l_1 .

We apply the Sokhotski-Plemelj formulas, the continuity principle and the generalized Liouville theorem on the torus \mathcal{R} to deduce the general solution to the Riemann-Hilbert problem (4.12)

$$\Phi(\zeta, u) = X(\zeta, u)[\Psi(\zeta, u) + \Omega(\zeta, u)], \quad (\zeta, u) \in \mathcal{R}. \quad (4.44)$$

Here, $\Omega(\zeta, u)$ is a rational function on the torus \mathcal{R} . Its form is determined from the following additional conditions the solution has to satisfy.

(i) Since the kernel dV has simple poles at the points $(\zeta_0, \pm u(\zeta_0))$ on both sheets of the surface \mathcal{R} , the function $\Psi(\zeta, u)$ has simple poles at these points. This gives simple poles to the function $\Phi(\zeta, u)$ which are unacceptable. To remove them, we admit that the function $\Omega(\zeta, u)$ also has simple poles at the points $(\zeta_0, \pm u(\zeta_0))$ and require that

$$\text{res}_{\zeta=\zeta_0} [\Psi(\zeta, u) + \Omega(\zeta, u)] = 0. \quad (4.45)$$

(ii) Owing to the simple pole of the function $X(\zeta, u)$ at the point $\mathbf{q}_1 = (\zeta_1, u(\zeta_1)) \in \mathcal{R}$, the function $\Psi(\zeta, u) + \Omega(\zeta, u)$ vanishes at this point,

$$\Psi(\zeta_1, u(\zeta_1)) + \Omega(\zeta_1, u(\zeta_1)) = 0. \quad (4.46)$$

(iii) Because of the simple zero of the function $X(\zeta, u)$ at the point $\mathbf{p}_1 = (\eta_1, u(\eta_1)) \in \mathbb{C}_1$, the function $\Omega(\zeta, u)$ has a simple pole at this point.

(iv) Since the functions $X(\zeta, u)$ and $\Psi(\zeta, u)$ are bounded at infinity and the function $\Phi(\zeta, u)$ has to be bounded, the function $\Omega(\zeta, u)$ must be bounded as $\zeta \rightarrow \infty$ as well.

(v) Owing to the symmetry of the functions $\Phi(\zeta, u)$, $X(\zeta, u)$, and $\Psi(\zeta, u)$, the function $\Omega(\zeta, u)$ has to be symmetric, $\Omega(\zeta, u) = \overline{\Omega(\zeta_*, u_*)}$.

The most general form of such a rational function is

$$\Omega(\zeta, u) = M_0 + (M_1 + iM_2) \frac{u(\zeta) + u(\eta_1)}{\zeta - \eta_1} - (M_1 - iM_2) \frac{u(\zeta) - u(\bar{\eta}_1)}{\zeta - \bar{\eta}_1}$$

$$+(M_3 + iM_4)\frac{u(\zeta) + u(\zeta_0)}{\zeta - \zeta_0} - (M_3 - iM_4)\frac{u(\zeta) - u(\zeta_0)}{\zeta - \zeta_0}, \quad (4.47)$$

where M_j ($j = 0, 1, \dots, 4$) are arbitrary real constants. This function satisfies the conditions (iii) and (v). Because of the growth of the function $u(\zeta)$ at infinity as $\zeta^{3/2}$, in general, the function $\Omega(\zeta, u)$ is unbounded at infinity. It becomes bounded and the condition (iv) is satisfied if

$$M_2 = -M_4. \quad (4.48)$$

To fulfill the property (i), that is to meet the condition (4.45), define the constants M_3 and M_4 as

$$M_3 = 0, \quad M_4 = \frac{\pi - \alpha}{4\pi} \int_{l'_0} \frac{d\zeta}{vX^+(\xi, v)}. \quad (4.49)$$

Finally, we make sure that the rational function $\Omega(\zeta, u)$ has property (ii). Denote

$$\begin{aligned} R + iJ &= \Psi(\zeta_1, u(\zeta_1)), \quad R_0 + iJ_0 = \frac{2u(\zeta_1)}{\zeta_1 - \zeta_0}, \\ R_1 + iJ_1 &= \frac{u(\zeta_1) + u(\eta_1)}{\zeta_1 - \eta_1}, \quad R_2 + iJ_2 = \frac{u(\zeta_1) - u(\bar{\eta}_1)}{\zeta_1 - \bar{\eta}_1}. \end{aligned} \quad (4.50)$$

where R , J , R_l , and J_l ($l = 0, 1, 2$) are real. Then equation (4.46) implies

$$M_1 = \frac{(R_0 - R_1 - R_2)M_2 - J}{J_1 - J_2},$$

$$M_0 = (R_2 - R_1)M_1 + (J_1 + J_2 - J_0)M_2 - R. \quad (4.51)$$

Having uniquely obtained all the five constants M_j ($j = 0, 1, \dots, 4$) in the rational function $\Omega(\zeta, u)$, we simplify it as

$$\Omega(\zeta, u) = M_0 + (M_1 + iM_2)\frac{u(\zeta) + u(\eta_1)}{\zeta - \eta_1} - (M_1 - iM_2)\frac{u(\zeta) - u(\bar{\eta}_1)}{\zeta - \bar{\eta}_1} - \frac{2iM_2u(\zeta)}{\zeta - \zeta_0} \quad (4.52)$$

and complete the solution procedure for the Riemann-Hilbert problem (4.12) by analyzing the behavior of the function $\Phi(\zeta, u)$ at the points a and ∞ .

Analysis of the integral $\Psi(\zeta, u)$ with the kernel dV as $\zeta \rightarrow a$ and $\zeta \rightarrow \bar{a}$ yields

$$\Psi(\zeta, u) \sim \frac{\pi - \alpha}{\sigma\pi i X^+(a, u(a))} \log(\zeta - a), \quad \zeta \rightarrow a, \quad \Psi(\zeta, u) \sim \text{const}, \quad \zeta \rightarrow \bar{a}, \quad (4.53)$$

where $\sigma = 1$ when $a \neq m$ and $\sigma = 2$ otherwise. Here, we took into account that the starting and terminal points of the contour l'_0 are $+\infty - i0$ and $a \in l_0^-$, respectively. Therefore, in virtue of (4.44), the function $\Phi(\zeta, u)$ has the logarithmic singularity, as $\zeta \rightarrow a$, and its asymptotics coincides with (4.15) predicted by employing formulas (2.5) and (2.6) and implementing asymptotic analysis of the conformal map $z = f(\zeta)$ in Section 3. As $\zeta \rightarrow \bar{a}$, the function $\Phi(\zeta, u)$ is bounded.

Analyze next the behavior of the functions $\Psi(\zeta, u)$ and $\Phi(\zeta, u)$ at infinity. By making the substitutions $\tau = 1/\xi$, $t = 1/\zeta$ we deduce as $\zeta \in l'_0 = (a, +\infty)^-$,

$$\Psi^+\left(\frac{1}{t}, u\left(\frac{1}{t}\right)\right) = \frac{\pi - \alpha}{X^+(1/t, u^-(1/t))} + \frac{\pi - \alpha}{2\pi i}(\mathcal{I}_1 + \mathcal{I}_2), \quad (4.54)$$

where

$$\mathcal{I}_1 = \int_0^{1/a} \frac{1 - t\zeta_0}{1 - \tau\zeta_0} \frac{d\tau}{(\tau - t)X^+(1/\tau, u^-(1/\tau))},$$

$$\mathcal{I}_2 = \int_0^{1/a} \sqrt{\frac{t(1-t)(1-mt)}{\tau(1-\tau)(1-m\tau)}} \frac{1-\tau\zeta_0}{1-t\zeta_0} \frac{d\tau}{(\tau-t)X^+(1/\tau, u^-(1/\tau))}. \quad (4.55)$$

As $t \rightarrow 0$ and $\zeta \in l'_0$, the integral \mathcal{I}_2 is bounded, whilst the integral \mathcal{I}_1 has a logarithmic singularity, and we have

$$\Psi^+(\zeta, u) \sim \frac{\pi - \alpha}{2\pi i X^+(+\infty - i0, u^-)} \log \zeta, \quad \zeta \rightarrow +\infty - i0, \quad (4.56)$$

where $X^+(+\infty - i0, u^-) = i|(\zeta_1 - \zeta_0)/(\eta_1 - \zeta_0)|$. It turns out that the principal term of the asymptotics of the function $\Psi(\zeta, u)$ as $\zeta \rightarrow +\infty + i0$ along the contour l'_0 is the same as in (4.56). In virtue of formula (4.44) we discover that $\Phi(\zeta, u) \sim (\pi - \alpha)/(2\pi i) \log \zeta$ as $\zeta \rightarrow \infty$ along the contour l_0 . This formula is identical to the asymptotics (4.14) obtained before by means of the asymptotic analysis of the conformal mapping in Section 3.

5 Exact representation of the conformal mapping $z = f(\zeta)$

The conformal mapping from the parametric domain \mathcal{D} onto the flow domain $\tilde{\mathcal{D}}$ is given by

$$f(\zeta) = i \int_a^\zeta \frac{N_0 + iN_1\xi}{p^{1/2}(\xi)} e^{-i\Phi^+(\xi, u(\xi))} d\xi, \quad \zeta \in \mathcal{D}, \quad (5.1)$$

The solution obtained has to satisfy two extra equations, the circulation condition (2.1) and the complex equation

$$\int_{l_1} \frac{df}{d\zeta} d\zeta = 0 \quad (5.2)$$

which guarantees that the conformal mapping is single-valued. Owing to formulas (2.5) and (2.6) we transform the circulation condition (2.1) into the form

$$\int_0^1 \frac{(N_0 + N_1\xi)d\xi}{\sqrt{|p(\xi)|}} = -\frac{\Gamma}{2U}. \quad (5.3)$$

This integral can be computed and expressed through the complete elliptic integrals of the first and second kind. We have

$$\begin{aligned} \int_0^1 \frac{d\xi}{\sqrt{|p(\xi)|}} &= 2k\mathbf{K}(k), \\ \int_0^1 \frac{\xi d\xi}{\sqrt{|p(\xi)|}} &= \frac{2}{k}[\mathbf{K}(k) - \mathbf{E}(k)], \quad k = \frac{1}{\sqrt{m}}. \end{aligned} \quad (5.4)$$

On substituting the integrals (5.4) into equation (5.3) we obtain a relation between the two real constants N_0 and N_1 ,

$$N_0 = -\frac{1}{k\mathbf{K}(k)} \left[\frac{\Gamma}{4U} + \frac{\mathbf{K}(k) - \mathbf{E}(k)}{k} N_1 \right]. \quad (5.5)$$

Transform now the second condition, equation (5.2). On substituting the representation (5.1) into equation (5.2) and denoting

$$c^\pm(\xi) = \cos[\Phi^+(\xi, u^\pm(\xi))], \quad s^\pm(\xi) = \sin[\Phi^+(\xi, u^\pm(\xi))], \quad \xi \in l_1^\pm, \quad (5.6)$$

we write equation (5.2) in the form

$$N_0 \int_0^1 \frac{c^+(\xi) + c^-(\xi) - is^+(\xi) - is^-(\xi)}{\sqrt{|p(\xi)|}} d\xi$$

$$+N_1 \int_0^1 \frac{c^+(\xi) + c^-(\xi) - is^+(\xi) - is^-(\xi)}{\sqrt{|p(\xi)|}} \xi d\xi = 0. \quad (5.7)$$

Note that since $\text{Im } \Phi^+(\xi, u^\pm(\xi)) = 0$ on l_0^\pm , the functions $c^\pm(\xi)$ and $s^\pm(\xi)$ are real-valued. On taking the real and imaginary parts of equation (5.7) we deduce

$$N_0 C_0 + N_1 C_1 = 0 \quad (5.8)$$

and

$$C_0 S_1 - C_1 S_0 = 0. \quad (5.9)$$

Here,

$$C_j = \int_0^1 \frac{c^+(\xi) + c^-(\xi)}{\sqrt{|p(\xi)|}} \xi^j d\xi, \quad S_j = \int_0^1 \frac{s^+(\xi) + s^-(\xi)}{\sqrt{|p(\xi)|}} \xi^j d\xi, \quad j = 0, 1. \quad (5.10)$$

Thus, in addition to equation (5.5) we obtained another equation for the constants N_0 and N_1 and we have

$$N_0 = - \left[1 - \frac{\mathbf{K}(k) - \mathbf{E}(k)}{k^2 \mathbf{K}(k)} \frac{C_0}{C_1} \right]^{-1} \frac{\Gamma}{4Uk\mathbf{K}(k)}, \quad N_1 = - \frac{N_0 C_0}{C_1}. \quad (5.11)$$

Equation (5.9) is a real transcendental equation for the two real parameters a and m . This enables us to conclude that the original problem possesses a one-parametric family of solutions provided equation (5.9) has a solution and it is unique.

6 Reconstruction of the vortex boundary and the wedge sides. Numerical results

The first step of the numerical procedure is to select a value of the parameter m and determine the parameter a by solving the transcendental equation (5.9). At this stage, we need to evaluate the integrals (5.10) whose integrands depend on the solution $\Phi^+(\xi, u)$ on the contour l_1 and are independent of the constants N_0 and N_1 . We note that we need the solution only on the first sheet. The function $\Phi^+(\xi, u)$ is given by (4.44) in terms of the factorization function $X(\zeta, u)$, the integral $\Psi(\zeta, u)$, and the rational function $\Omega(\zeta, u)$. The factorization function depends on the point \mathbf{q}_1 and the integer n_a , the solution to the Jacobi inversion problem. It turns out that for all realistic values of the problem parameters used in the numerical tests and when $\mathbf{p}_1 = (\eta_1, u(\eta_1)) \in \mathbb{C}_1$, the point $\mathbf{q}_1 = (\zeta_1, u(\zeta_1))$ also lies in the upper sheet \mathbb{C}_1 , and $n_a = 0$. We remark that the final solution, the conformal map $z = f(\zeta)$, is independent of not only the point \mathbf{p}_1 but also the real point $\zeta_0 < 0$.

Describe first the algorithm for the function $X(\zeta, u)$. It is convenient to write it in the form

$$X(\zeta, u) = \lambda \exp \left\{ \frac{u(\zeta)}{i(\zeta - \zeta_0)} \left(\frac{1}{2} - 2n_a \right) \mathcal{J}_1(\zeta) - \frac{\mathcal{J}_2(\zeta, u) + \mathcal{J}_3(\zeta, u)}{2} \right\}, \quad (6.1)$$

where $\lambda = 1$ if $(\zeta, u) \in \mathbb{C}_1 \setminus l_0$, $\lambda = i$ if $(\zeta, u) \in l_0 \subset \mathbb{C}_1$,

$$\mathcal{J}_1(\zeta) = \int_m^\infty \frac{(\xi - \zeta_0)d\xi}{\sqrt{\xi(\xi - 1)(\xi - m)(\xi - \zeta)}},$$

$$\mathcal{J}_2(\zeta, u) = \int_\gamma \left(\frac{\zeta - \zeta_0}{\xi - \zeta_0} + \frac{u(\zeta)}{u(\xi)} \frac{\xi - \zeta_0}{\zeta - \zeta_0} \right) \frac{d\xi}{\xi - \zeta}, \quad \mathcal{J}_3(\zeta, u) = \int_\gamma \left(\frac{\zeta - \zeta_0}{\bar{\xi} - \zeta_0} - \frac{u(\zeta)}{u(\bar{\xi})} \frac{\bar{\xi} - \zeta_0}{\zeta - \zeta_0} \right) \frac{d\bar{\xi}}{\bar{\xi} - \zeta}. \quad (6.2)$$

Analyze the first integral. If $\zeta \notin (m, +\infty)$, by making the substitution $\xi = 1/\tau$ we obtain

$$\mathcal{J}_1(\zeta) = \frac{1}{\sqrt{m}} \int_0^{1/m} \frac{\mathcal{F}_1(\tau)d\tau}{\sqrt{\tau(1/m - \tau)}}, \quad \mathcal{F}_1(\tau) = \frac{1 - \zeta_0\tau}{\sqrt{1 - \tau(1 - \tau\zeta)}}. \quad (6.3)$$

By employing the integration formula with the Gaussian weights π/n and the abscissas $x_j = \cos(j - \frac{1}{2})\frac{\pi}{n}$ we write approximately

$$\mathcal{J}_1(\zeta) \approx \frac{\pi}{\sqrt{mn}} \sum_{j=1}^n \mathcal{F}_1\left(\frac{1+x_j}{2m}\right). \quad (6.4)$$

When $\zeta \in (m, +\infty)$, the integral $\mathcal{J}_1(\zeta)$ is singular, and its Cauchy principal value is computed by [1]

$$\mathcal{J}_1(\zeta) = -\frac{2\pi\sqrt{m}}{\zeta} \sum_{s=1}^{\infty} d'_s U_{s-1}\left(\frac{2m}{\zeta} - 1\right), \quad (6.5)$$

where

$$d'_s = \frac{2}{\pi} \int_{-1}^1 \tilde{\mathcal{F}}_1\left(\frac{1+\tau}{2m}\right) \frac{T_s(\tau)d\tau}{\sqrt{1-\tau^2}} \approx \frac{2}{n} \sum_{j=1}^n \tilde{\mathcal{F}}_1\left(\frac{1+x_j}{2m}\right) \cos\left(j - \frac{1}{2}\right) \frac{s\pi}{n}, \quad s = 1, 2, \dots \quad (6.6)$$

$\tilde{\mathcal{F}}_1(\tau) = (1 - \tau\zeta_0)(1 - \tau)^{-1/2}$, and $T_s(\tau)$ and $U_s(\tau)$ are the Chebyshev polynomials. Our numerous tests reveal that if $\text{Im}\eta_1$ is chosen to be positive, then $\text{Im}\zeta_1 < 0$. It is convenient to split the contour γ lying in the upper sheet into two segments (η_1, δ) and (δ, ζ_1) , $\zeta_0 < \delta < 0$. This leads to the following representations of the integrals \mathcal{J}_2 and \mathcal{J}_3 :

$$\mathcal{J}_2(\zeta, u) = j^+(\zeta, u; \zeta_1) - j^+(\zeta, u; \eta_1), \quad \mathcal{J}_3(\zeta, u) = j^-(\zeta, u; \bar{\zeta}_1) - j^-(\zeta, u; \bar{\eta}_1), \quad (6.7)$$

where $j^{\pm}(\zeta, u; \eta)$ are the integrals

$$j^{\pm}(\zeta, u; \eta) = \int_{\delta}^{\eta} \left(\frac{\zeta - \zeta_0}{\xi - \zeta_0} \pm \frac{u(\zeta)}{u(\xi)} \frac{\xi - \zeta_0}{\zeta - \zeta_0} \right) \frac{d\xi}{\xi - \zeta} \quad (6.8)$$

evaluated by the Gauss quadrature formula employed for the integral (6.3).

Consider next the function $\Psi(\zeta, u)$. If $\zeta \notin l'_0 = (a, +\infty)^-$, then the integral is not singular. On making the substitution $\xi = 1/\tau$, we recast it into

$$\Psi(\zeta, u) = -\frac{\pi - \alpha}{2\pi i} \int_0^{1/a} \frac{\mathcal{F}_*(\zeta, u; \tau)d\tau}{\sqrt{\tau(1/a - \tau)}}, \quad (6.9)$$

where

$$\mathcal{F}_*(\zeta, u; \tau) = \left(\frac{(\zeta - \zeta_0)\sqrt{\tau}}{1 - \tau\zeta_0} - \frac{u(\zeta)(1 - \zeta_0\tau)}{i\sqrt{(1 - \tau)(1 - m\tau)}(\zeta - \zeta_0)} \right) \frac{\sqrt{1/a - \tau}}{(1 - \tau\zeta)X^+(1/\tau, v^-)}, \quad (6.10)$$

where $v^- = u(\xi - i0)$. This integral is efficiently evaluated by the Gauss quadrature formulas used in (6.3), where m and \mathcal{F}_1 need to be replaced by a and \mathcal{F}_* , respectively.

In the case $\zeta \in l'_0 = (a, +\infty)^-$ on the upper sheet, the integral $\Psi(\zeta, u)$ is singular. We denote $u^- = u(\zeta)$, $\zeta \in l'_0$, and by the Sokhotski-Plemelj formulas,

$$\Psi^+(\zeta, u^-) = \frac{\pi - \alpha}{X^+(\zeta, u^-)} + \Psi(\zeta, u^-), \quad \zeta \in l'_0. \quad (6.11)$$

We again use the formula [1] for the Cauchy principal value $\Psi(\zeta, u^-)$ and similar to the integral \mathcal{J}_1 obtain

$$\Psi(\zeta, u^-) = \frac{\pi - \alpha}{2\pi i} \int_0^{1/a} \frac{\mathcal{F}(\tau)d\tau}{\sqrt{\tau(1/a - \tau)}(\tau - t)} = -i(\pi - \alpha)a \sum_{s=1}^{\infty} d_s U_{s-1}\left(\frac{2a}{\zeta} - 1\right), \quad (6.12)$$

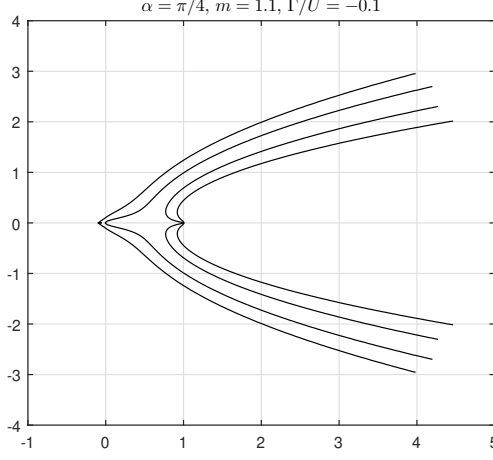


Figure 3: The preimages of some streamlines when $\alpha = \pi/4$, $\Gamma/U = -0.1$, $m = 1.1$.

where $t = 1/\zeta$, $\zeta = l'_0$,

$$\mathcal{F}(\tau) = \left[\frac{(1 - \zeta_0 t)\sqrt{\tau}}{1 - \zeta_0 \tau} + \sqrt{\frac{t(1-t)(1-mt)}{(1-\tau)(1-mt)}} \frac{1 - \zeta_0 \tau}{1 - \zeta_0 t} \right] \frac{\sqrt{1/a - \tau}}{X^+(1/\tau, v^-)}.$$

$$d_s \approx \frac{2}{n} \sum_{j=1}^n \mathcal{F}\left(\frac{1+x_j}{2a}\right) \cos\left(j - \frac{1}{2}\right) \frac{s\pi}{n}, \quad s = 1, 2, \dots \quad (6.13)$$

Note that according to (4.56) the series in (6.12) has a logarithmic singularity as $\zeta \rightarrow \infty$.

The third function in the representation (4.44) of the solution of the Riemann-Hilbert problem, the function $\Omega(\zeta, u)$, has three real constants M_0 , M_1 , and M_2 . The constant M_2 is the integral

$$M_2 = -\frac{\pi - \alpha}{4\pi} \int_{l'_0} \frac{d\xi}{v^- X^+(\xi, v^-)} = -\frac{\pi - \alpha}{4\pi i} \int_0^{1/a} \frac{\mathcal{F}_0(\tau) d\tau}{\sqrt{\tau(1/a - \tau)}}, \quad (6.14)$$

where

$$\mathcal{F}_0(\tau) = \frac{\sqrt{1/a - \tau}}{\sqrt{(1-\tau)(1-m\tau)} X^+(1/\tau, v^-)}. \quad (6.15)$$

This integral is evaluated numerically by the Gauss quadrature rule employed before. The other two constants are expressed through M_2 by (4.51).

Having equipped with formulas for $\Phi^+(\xi, u)$ efficient for numerical purposes, we can evaluate the integrals (5.10) by applying the Gauss quadratures and solve the transcendental equation (5.9). It turns out that, for all numerical tests implemented, $a = m$. In the following formulas we do not distinguish the points a and m anymore.

We aim now to show that the conformal map we found indeed maps the contours l_0^- and l_0^+ into the sides $\arg z = \alpha$ and $\arg z = 0$ of the wedge, respectively. Let $\zeta \in l_0^\pm$. Then

$$f(\zeta) = \pm \int_m^\zeta \frac{N_0 + N_1 \xi}{\sqrt{|p(\xi)|}} e^{-i\Phi^+(\xi, v^\pm)} d\xi \quad v^\pm = u(\xi^\pm). \quad (6.16)$$

Notice that on both sides l_0^\pm of the contour l_0 , $\operatorname{Re} X^+(\xi, v^\pm) = 0$, $\operatorname{Im} \Omega(\xi, v^\pm) = 0$. Owing to formula (6.11), we discover

$$\Phi^+(\xi, v^-) = \pi - \alpha + iP(\xi, v^-), \quad \xi \in l_0^-, \quad \Phi^+(\xi, v^+) = iP(\xi, v^+), \quad \xi \in l_0^+, \quad (6.17)$$

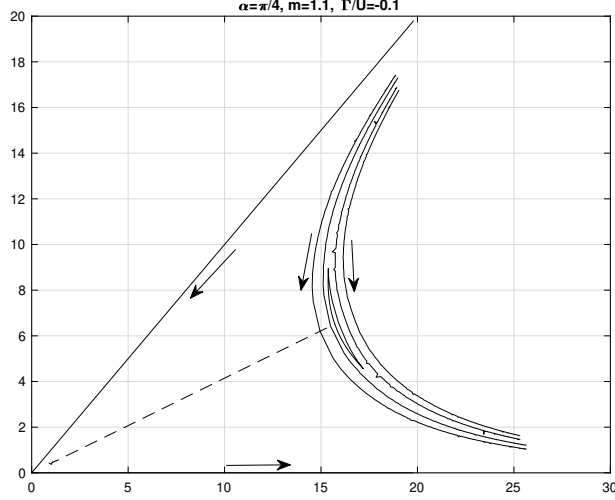


Figure 4: The vortex domain and some streamlines when $\alpha = \pi/4$, $\Gamma/U = -0.1$, $m = 1.1$.

Here, $P(\xi, v^\pm)$ are real-valued functions,

$$P(\xi, v^\pm) = \text{Im } X^+(\xi, v^\pm)[\Psi(\xi, v^\pm) + \Omega(\xi, v^\pm)], \quad \xi \in l_0^\pm. \quad (6.18)$$

Returning to equation (6.16), we deduce

$$f(\zeta) = e^{i\alpha} \int_m^\zeta \frac{N_0 + N_1\xi}{\sqrt{|p(\xi)|}} e^{P(\xi, v^-)} d\xi, \quad \zeta \in l_0^-, \quad f(\zeta) = \int_m^\zeta \frac{N_0 + N_1\xi}{\sqrt{|p(\xi)|}} e^{P(\xi, v^+)} d\xi, \quad \zeta \in l_0^+. \quad (6.19)$$

Our numerical tests show that the function $N_0 + N_1\xi$ is positive for all $\xi \in (m, +\infty)$. This implies that $z = f(\zeta)$ maps the contours l_0^- and l_0^+ into the sides AB and AC of the wedge, respectively.

To reconstruct the vortex boundary, we shall determine the image of the straight path joining the starting point $\zeta = m$ and the terminal point $\zeta = 1$. Analysis of the factorization function $X(\zeta, u)$ and $\Psi(\zeta, u)$ given by (6.1) and (4.43) shows that both functions have singularities as $\zeta \rightarrow m^-$. To determine the position of the image of the point $\zeta = 1$ with a good accuracy is crucial for the algorithm capability to reconstruct the vortex profile and streamlines close to the vortex. Consider the singular integral $\mathcal{J}_1(\zeta)$ that brings the singularity to the function $X(\zeta, u)$. Denote $t = 1/\zeta$ and for $1/m < t < 1$ we have

$$\mathcal{J}_1(\zeta) = \mathcal{J}_1^*(t) + \mathcal{J}_1^{**}(t), \quad (6.20)$$

where

$$\begin{aligned} \mathcal{J}_1^*(t) &= -t \int_0^{1/m} \left(\frac{1 - \zeta_0\tau}{\sqrt{1 - \tau}} - \frac{1 - \zeta_0/m}{\sqrt{1 - 1/m}} \right) \frac{d\tau}{\sqrt{\tau(1 - m\tau)}(\tau - t)}, \quad \frac{1}{m} < t < 1. \\ \mathcal{J}_1^{**}(t) &= -t \frac{1 - \zeta_0/m}{\sqrt{1 - 1/m}} \int_0^{1/m} \frac{d\tau}{\sqrt{\tau(1 - m\tau)}(\tau - t)}, \quad \frac{1}{m} < t < 1. \end{aligned} \quad (6.21)$$

The first integral is not singular, and we can manage with it using the Gauss quadrature rule, whilst the second integral that carries the singularity is evaluated exactly,

$$\mathcal{J}_1^{**}(t) = \frac{1 - \zeta_0/m}{\sqrt{1 - 1/m}} \frac{\pi t}{\sqrt{t(mt - 1)}}, \quad \frac{1}{m} < t < 1. \quad (6.22)$$

By passing to the limit $\zeta \rightarrow m^-$ and $\zeta \rightarrow m^+ \pm i0$ in (6.1) and using formula (6.22) we obtain

$$\lim_{\zeta \rightarrow m^+ \pm i0} X^+(\xi, v) = \lim_{\zeta \rightarrow m^-} X(\zeta, u) = X(m, u) = i \left| \frac{(\zeta_1 - \zeta_0)(\eta_1 - m)}{(\zeta_1 - m)(\eta_1 - \zeta_0)} \right|. \quad (6.23)$$

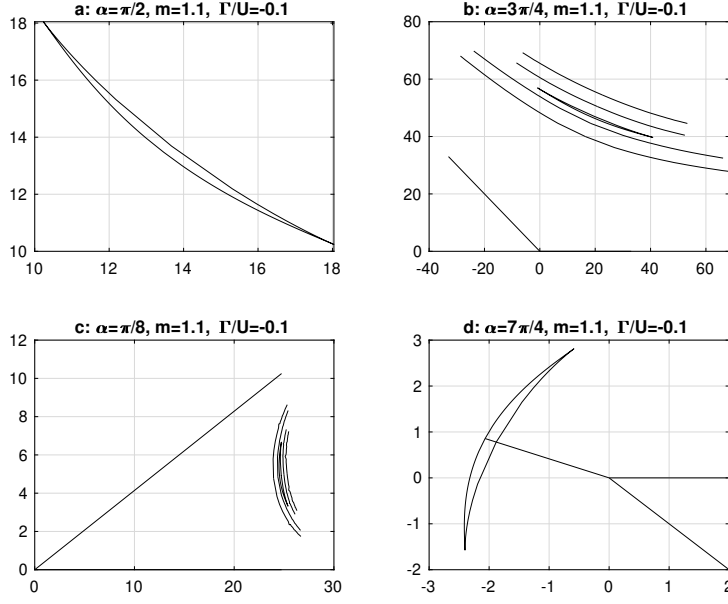


Figure 5: The vortex domain, the wedge, and some streamlines for $m = 1.1$ when (a) $\alpha = \frac{1}{2}\pi$, (b) $\alpha = \frac{3}{4}\pi$, (c) $\alpha = \frac{1}{8}\pi$, (d) $\alpha = \frac{7}{4}\pi$: owing to penetration of streamlines into the vortex domain the solution does not exist for $\alpha > \pi$.

Consider next the function $\Psi(\zeta, u)$ with $(\zeta, u) \in \mathbb{C}_1$. For $\zeta = 1/t \in (1, m)$ we represent it in the form

$$\Psi(\zeta, u) = \Psi_1(t) + \Psi_2(t), \quad (6.24)$$

where

$$\begin{aligned} \Psi_1(t) &= \Psi_1^*(t) + \frac{\pi - \alpha}{2\pi i X(m, u)} \log \frac{t - 1/m}{t}, \\ \Psi_2(t) &= -\frac{(\pi - \alpha)\sqrt{1-t}}{2(1-\zeta_0 t)} \left[\frac{\sqrt{t(1-mt)}}{\pi} \Psi_2^*(t) - r_0 \right], \quad r_0 = \frac{1 - \zeta_0/m}{\sqrt{1 - 1/m} X(m, u)}. \end{aligned} \quad (6.25)$$

The integrals $\Psi_1^*(t)$ and $\Psi_2^*(t)$ are given by

$$\begin{aligned} \Psi_1^*(t) &= \frac{\pi - \alpha}{2\pi i} \int_0^{1/m} \left[\frac{1 - \zeta_0 t}{(1 - \zeta_0 \tau) X^+(1/\tau, v)} - \frac{1}{X(m, u)} \right] \frac{d\tau}{\tau - t}, \\ \Psi_2^*(t) &= \int_0^{1/m} \left[\frac{1 - \zeta_0 \tau}{\sqrt{1 - \tau} X^+(1/\tau, v)} - r_0 \right] \cdot \frac{d\tau}{\sqrt{\tau(1-m\tau)}(\tau - t)}. \end{aligned} \quad (6.26)$$

They are evaluated numerically in the same manner as before since they are not singular. On combining these formulas we obtain for $\zeta < m$ close to m

$$\Psi(\zeta, u) \sim \frac{\pi - \alpha}{2\pi i X(m, u)} \log(m - \zeta) + \frac{\Lambda_0}{iX(m, u)}, \quad \zeta \rightarrow m^-, \quad (6.27)$$

where

$$\Lambda_0 = \frac{\pi - \alpha}{2} \left(i - \frac{\log m}{\pi} \right) + iX(m, u)\Psi_1^*(1/m). \quad (6.28)$$

From here we discover the asymptotics of the solution $\Phi(\zeta, u)$ to the Riemann-Hilbert problem (4.12) on the first sheet \mathbb{C}_1 and of the corresponding function $\exp\{-i\Phi(\zeta, u)\}$

$$\Phi(\zeta, u) \sim \frac{\pi - \alpha}{2\pi i} \log(m - \zeta) - i\Lambda_0 + X(m, u)\Omega(m, u),$$

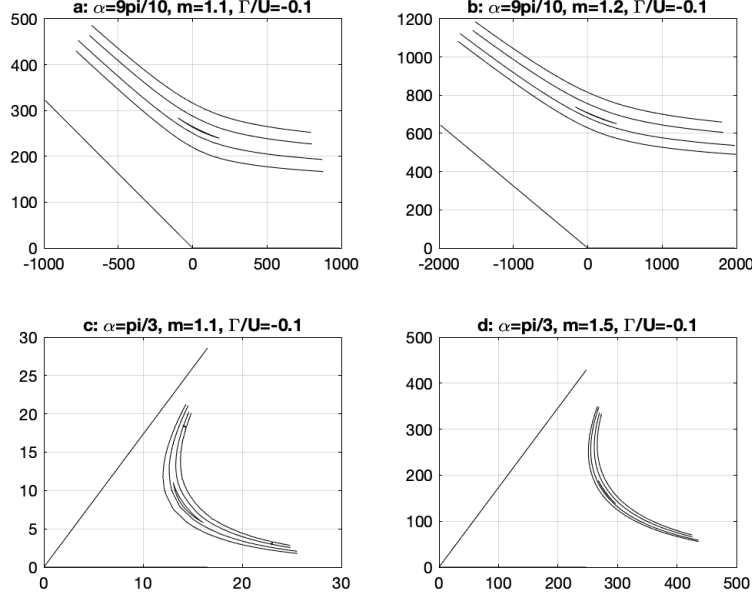


Figure 6: The vortex domain, the wedge, and some streamlines when (a) $\alpha = \frac{9}{10}\pi$, $m = 1.1$ (b) $\alpha = \frac{9}{10}\pi$, $m = 1.2$ (c) $\alpha = \frac{1}{3}\pi$, $m = 1.1$, d) $\alpha = \frac{1}{3}\pi$, $m = 1.5$.

$$e^{-i\Phi(\zeta, u)} \sim (m - \zeta)^{-1/2 + \alpha/(2\pi)} \Lambda_1, \quad \zeta \rightarrow m^-. \quad (6.29)$$

Here,

$$\Lambda_1 = e^{-\Lambda_0 - iX(m, u)\Omega(m, u)}. \quad (6.30)$$

The images $f(\zeta)$ of the points $\zeta \in [1, m]$ can now be evaluated with a good accuracy by applying the formula

$$f(\zeta) = i \int_{\zeta}^m \frac{g(\xi) d\xi}{\sqrt{(m - \xi)(\xi - \zeta)}} + \frac{2\pi i N}{\alpha} (m - \zeta)^{\alpha/(2\pi)}, \quad 1 \leq \zeta \leq m, \quad (6.31)$$

where

$$g(\xi) = \frac{(N_0 + N_1 \xi) e^{-i\Phi(\xi, u)}}{\sqrt{\xi(\xi - 1)}} - N(m - \xi)^{-1/2 + \alpha/(2\pi)}, \quad N = \frac{(N_0 + N_1 m) \Lambda_1}{\sqrt{m(m - 1)}}. \quad (6.32)$$

Since the function $g(\xi)$ is not singular at the point m , $g(\xi) = O((m - \xi)^{1/2 + \alpha/(2\pi)})$, $\xi \rightarrow m$, the integral in (6.31) is evaluated by the Gauss quadrature formula.

At the final step of the procedure we determine the profile $z = f(\zeta)$ of the vortex domain by employing the formula

$$f(\zeta^{\pm}) = f(1) \mp \int_1^{\zeta^{\pm}} \frac{(N_0 + N_1 \xi) e^{-i\Phi^+(\xi^{\pm}, v^{\pm})} d\xi}{\sqrt{\xi(1 - \xi)(m - \xi)}}, \quad \xi^{\pm}, \zeta^{\pm} \in l_1^{\pm}, \quad (6.33)$$

and the velocity on the wedge walls

$$\frac{dw}{Udz} = \frac{u_x - iu_y}{U} = \lambda^{\pm} \exp \{X^+(\xi^{\pm}, v^{\pm})[\Psi(\xi^{\pm}, v^{\pm}) + \Omega(\xi^{\pm}, v^{\pm})]\}, \quad \xi^{\pm} \in l_0^{\pm}, \quad (6.34)$$

where $v^{\pm} = u(\xi^{\pm})$, $\lambda^+ = 1$ as $\xi \in l_0^+$ ($z \in AC$) and $\lambda^- = e^{i(\pi - \alpha)}$ as $\xi \in l_0^-$ ($z \in AB$). The complex constant $f(1)$ is computed from (6.31), and the nonsingular integral (6.33) is evaluated by the Gauss

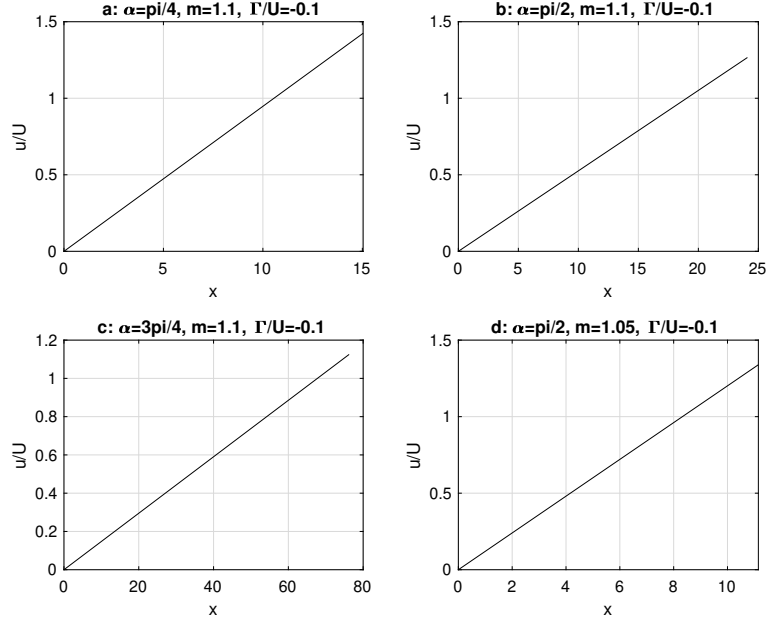


Figure 7: The normalized tangential velocity u_x/U on the horizontal side of the wedge when $\Gamma/U = -0.1$ (a) $\alpha = \frac{1}{4}\pi$, $m = 1.1$ (b) $\alpha = \frac{1}{2}\pi$, $m = 1.1$ (c) $\alpha = \frac{3}{4}\pi$, $m = 1.1$, d) $\alpha = \frac{1}{2}\pi$, $m = 1.05$.

formula in a simple manner. It is directly verified that the argument of the exponential function in (6.34) is real, and the boundary conditions (2.2) are satisfied. Analysis of the asymptotics of the functions $\Psi(\xi^\pm, v^\pm)$ as $\xi^\pm \rightarrow m$ yields

$$\Psi(\xi^\pm, v^\pm) \sim \frac{\pi - \alpha}{2\pi i X(m, u)} \log(\xi - m), \quad \xi^\pm \rightarrow m, \quad (6.35)$$

and therefore

$$\frac{dw}{Udz} \sim K(\xi - m)^{1/2 - \alpha/(2\pi)}, \quad \xi \rightarrow m, \quad \xi \in l_0^\pm, \quad K = \text{const}. \quad (6.36)$$

This implies $dw/dz \sim cz^{\pi/\alpha - 1}$, $z \rightarrow 0$, that is consistent with the analysis of Section 4.1 in the case $a = m$.

For numerical tests, we select $\zeta_0 = -5$, $\delta = -2$, and $\eta_1 = 1 + i/2$. We emphasize that all the curves presented in Figures 3 to 7 are independent of the choice of these parameters provided $-\infty < \zeta_0 < \delta < 0$ and $\text{Im } \eta_1 \neq 0$. In the case $m = 1.1$, the output of the Jacobi inversion problem is $n_a = n_b = 0$ and $\zeta_1 = 0.668204 - 0.835295i \in \mathbb{C}_1$. For all other values of the parameters we tested, the situation is similar: $n_a = n_b = 0$ and $\zeta_1 \in \mathbb{C}_1$ with $\text{Im } \zeta_1 < 0$.

The only one restriction for the parameter Γ/U is it has to be negative. If it is positive, then the model problem (2.1) to (2.4) is solvable if the direction of the velocity on the wedge walls is reversed and the boundary condition (2.2) is changed accordingly. Otherwise the solution does not exist. The parameter Γ/U is selected to be -0.1 for all our tests. The preimages

$$\text{Im} \int_{\xi_0}^{\zeta} \omega_0(\eta) d\eta = 0 \quad (6.37)$$

in the ζ -parametric plane of some streamlines around the vortex are presented in Fig.3. Here, $\omega_0(\eta)$ is given by (3.2), $\xi_0 < 0$ for the preimages of streamlines facing the infinite point of the wedge and $1 < \xi_0 < m$ of those facing the corner. The curves are symmetric with respect to the real axis. In Fig.3, the point ξ_0 is chosen to be -0.01 , -0.05 and 1.001 , 1.01 , respectively, while $\alpha = \frac{1}{4}\pi$ and

$m = 1.1$. The vortex and the streamlines corresponding to their preimages in Fig. 3 for the same α and m are shown in Fig. 4. Two cusps are seen at the points where the streamline branches and where the branches merge. The dashed line demonstrates the preimage of the straight path from m to 1. Figures 5 a-b show the vortex domains and in cases b and c some streamlines around the vortex when $m = 1.1$ and the angle $\alpha = \frac{1}{2}\pi$ (a), $\alpha = \frac{3}{4}\pi$ (b), and $\alpha = \frac{1}{8}\pi$ (c). It turns out that for angles $\alpha > \pi$ the preimage of the straight path from $\zeta = m$ to $\zeta = 1$ intersects the preimage of the contour l_1 (Fig. 5 d). It is also found that the streamlines close to the vortex boundary penetrate it. These results indicate that a vortex domain with the prescribed properties does not exist in wedges when $\alpha > \pi$. Some other samples of vortices and streamlines nearby are given in Fig. 6 a-d. In Fig. 6 a and b, $\alpha = \frac{9}{10}\pi$ with $m = 1.1$ and $m = 1.2$. In Fig. 6 c and d, $\alpha = \frac{1}{3}\pi$ with $m = 1.1$ and $m = 1.5$. It is seen that when the conformal mapping free parameter m grows the vorticity drifts out of the wedge corner. Fig. 6 a and b also show that when α grows and approaches π , the vortex sheet length grows as well, and the vortex domain moves away from the corner. The normalized tangential velocity u_x/U on the horizontal side of the wedge is plotted for some α and m in Fig. 7. It is seen that when the angle α decreases, the speed u_x is increasing. It is also observed that when m decreases and the vortex becomes closer to the corner, the speed grows.

7 Conclusions

A two-dimensional flow of an inviscid incompressible fluid in a wedge with impenetrable walls about a Sadvskii vortex has been investigated by the method of conformal mappings. The shape of the vortex domain is unknown *a priori*, and no stagnation points on the wedge sides are admitted by the model. The map has been constructed by solving a symmetric Riemann-Hilbert problem on a finite and a semi-infinite segments lying on an elliptic Riemann surface. Owing to the asymptotics at infinity of the classical Weierstrass analogue of the Cauchy kernel for an elliptic surface and the right hand-side of the Riemann-Hilbert problem, the use of the Weierstrass kernel leads to divergent integrals. A new analogue of the Cauchy kernel on a hyperelliptic surface with properties required has been proposed, and a closed-form solution to the Riemann-Hilbert problem has been constructed. It is noted that the Weierstrass kernel would have worked if another map from the exterior of two finite segments on the flow domain had been applied. The initial authors' efforts to numerically implement the procedure and recover such a map failed. On the contrary, the mapping from a finite and a semi-infinite two-sided segments onto the vortex boundary and the wedge walls, respectively, has been numerically successful. The conformal mapping recovered by solving the Riemann-Hilbert problem has a free geometric parameter and two problem parameters, the wedge angle α and the ratio Γ/U of the circulation and the speed on the vortex boundary. The vortex and the wedge boundaries have been determined by quadratures and numerically reconstructed. The vortex boundary formed by two branches of the same streamline in all numerical tests share the same feature of having two cusps. It has also been found that although for the wedge angle α greater than π , it is possible to reconstruct a vortex domain by solving the free boundary problem, the solution cannot be accepted as a physical one since streamlines close to the vortex domain penetrate the vortex interior. Thus the solution exists and has one free real parameter for $\alpha < \pi$ and does not exist when $\alpha > \pi$.

Acknowledgments.

The authors thank the Isaac Newton Institute for Mathematical Sciences, Cambridge, for support and hospitality during the program Complex analysis: techniques, applications and computations, where a part of work on this paper was undertaken.

References

- [1] Y.A. ANTIPOV, *Method of Riemann surfaces for an inverse antiplane problem in an n -connected domain*, Complex Var. Elliptic Equ., **65** (2020), pp. 455-480.
- [2] Y.A. ANTIPOV AND V.V. SILVESTROV, *Method of Riemann surfaces in the study of supercavitating flow around two hydrofoils in a channel*, Phys. D, **235** (2007), pp. 72-81.
- [3] Y.A. ANTIPOV AND V.V. SILVESTROV, *Double cavity flow past a wedge*, Proc. R. Soc. A., **464** (2008), pp. 3021-3038.
- [4] Y.A. ANTIPOV AND A.Y. ZEMLYANOVA, *Motion of a yawed supercavitating wedge beneath a free surface*, SIAM J. Appl. Math., **70** (2009), pp. 923-948.
- [5] Y.A. ANTIPOV AND A.Y. ZEMLYANOVA, *Single- and double-spiral-vortex models for a supercavitating non-symmetric wedge in a jet*, Proc. R. Soc. A., **465** (2009), pp. 3817-3837.
- [6] G. BIRKHOFF AND E. H. ZARANTONELLO, *Jets, Wakes, and Cavities*, Academic Press, New York, 1957.
- [7] G.R. BAKER, P.G. SAFFMAN, AND J.S. SHEFFIELD, *Structure of a linear array of hollow vortices of finite cross-section*, J. Fluid Mech., **74**(3) (1976), pp. 469-476.
- [8] T.W. CHRISTOPHER AND S.G. LLEWELLYN SMITH, *Hollow vortex in a corner*, J. Fluid Mech., **908** (2021), R2 1-12.
- [9] D. CROWDY, *Solving Problems in Multiply Connected Domains*, SIAM, Philadelphia, 2020.
- [10] J. D. ESHELBY *The determination of the elastic field of an ellipsoidal inclusion, and related problems*, Proc. Roy. Soc. London A 241 (1957), pp. 376-396.
- [11] B. GUSTAFSSON AND A. VASIL'EV, *Conformal and potential analysis in Hele-Shaw cells*, Advances in Mathematical Fluid Mechanics. Birkhäuser Verlag, Basel, 2006
- [12] A.R. LOW, *Normal Elliptic Functions*, University of Toronto Press, Toronto, 1950.
- [13] D.W. MOORE, P.G. SAFFMAN, S. TANVEER, *The calculation of some Batchelor flows: the Sadovskii vortex and rotational corner flow*, Phys. Fluids, **31** (1988), pp. 978-990.
- [14] H.C. POCKLINGTON, *The configuration of a pair of equal and opposite hollow straight vortices, of finite cross-section, moving steadily through fluid*, Proc. Cambridge Philos. Soc., **8** (1895), 178-187.
- [15] V.S. SADOVSKII, *Vortex regions in a potential stream with a jump of Bernoulli's constant at the boundary*, J. Appl. Math. Mech. (PMM), **35** (1971), pp. 729-735.
- [16] P.G. SAFFMAN, *Vortex Dynamics*, Cambridge University Press, Cambridge, 1992.
- [17] R. VAGLIO-LAURIN AND M. H. BLOOM, *Chemical effects in external hypersonic flows*. In Hypersonic Flow Research, Ed. F.R. Riddell, Academic Press, New York, 1962.
- [18] A.Y. ZEMLYANOVA AND Y.A. ANTIPOV, *Single-spiral-vortex model for a cavitating elastic curvilinear foil*, SIAM J. Appl. Math., **72** (2012), pp. 280-298.
- [19] E. I. ZVEROVICH, *Boundary value problems in the theory of analytic functions in Hölder classes on Riemann surfaces*, Russian Math. Surveys, **26** (1971), pp. 117-192,